Intertwined Rashba, Dirac and Weyl Fermions in Hexagonal Hyperferroelectrics: Supplementary Material

Domenico Di Sante,[1,2] Paolo Barone,[1] Alessandro Stroppa,[1] Kevin F. Garrity,[3] David Vanderbilt,[4] and Silvia Picozzi[1]

[1] *Consiglio Nazionale delle Ricerche (CNR-SPIN), Via Vetoio, L'Aquila, Italy**

[2] *Department of Physical and Chemical Sciences, University of L'Aquila, Via Vetoio 10, I-67010 L'Aquila, Italy*

[3] *Material Measurement Laboratory, National Institute of Standards and Technology, Gaithersburg MD, 20899, USA*

[4] *Department of Physics and Astronomy, Rutgers University, Piscataway, New Jersey 08854, USA*

(Dated: January 3, 2016)

COMPUTATIONAL METHODS

We performed first-principles calculations using the projector augmented plane wave method as implemented in Vienna Ab-initio Simulation Package (VASP) [1]. We adopted the Heyd-Scuseria-Ernzerhof (HSE) hybrid functional for the exchange-correlation part[2], while SOC has been included self-consistently in a scalar-relativistic scheme. We used a plane wave cutoff of 600 eV on a $8 \times 8 \times 8$ Monkhorst-Pack k-point mesh. Atomic positions and structural parameters for NaZnSb and KMgBi, the two prototypical systems investigated in our work, were taken from TABLE III of Ref. [3]. Furthermore, we used a basis of K $4s$, Mg $3s$ and Bi $6s$, $6p$ orbitals for constructing Wannier functions [4]. The obtained tight-binding parameters were used to study slab geometries and semi-infinite slabs, to calculate topological invariants, and to investigate the role of disorder in alloys. Surface spectral functions have been computed within the surface renormalization scheme [5]. Surface states in slab geometry, on the other hand, have been calculated by solving the tight-binding model in slabs comprising up to 100 K and [MgBi] layers.

The Z_2 topological invariants $(\nu_0;\nu_1,\nu_2,\nu_3)$ characteristic of 3D topological insulators have been calculated following the general method proposed in Ref.[6], which is applicable to noncentrosymmetric materials. Considering the rhomboid defined in the Brillouin zone, whose vertices are the 8 time-reversal-invariant momenta $\Gamma(n_1,n_2,n_3) = 0.5(n_1\boldsymbol{b}_1 + n_2\boldsymbol{b}_2 + n_3\boldsymbol{b}_3)$ (being $\boldsymbol{b}_i$ the reciprocal lattice vectors and $n_i = 0,1$), one defines six tori spanned by reciprocal lattice vectors $\{b_1,b_2\}$, $\{b_2,b_3\}$ and $\{b_1,b_3\}$, with the third component fixed by $n_i = 0,1$ (where $i = 3,1,2$, respectively). The Z_2 invariants can be deduced enforcing the analogy with the adiabatic charge pumping within each half-torus, at whose edge degenerate Kramer's pairs are due to appear because of the time-reversal symmetry. [7, 8] We calculate the one-dimensional Wannier charge centers (WCC) from the Bloch states of occupied bands within each half-torus (shown in Suppl. Fig. 3), where one component of the k vector is treated as an effective adiabatic pumping parameter, and then we track the midpoint of the largest gap between the adjacent WCCs. If the midpoint of this largest gap jumps over an odd number of WCCs during the effective adiabatic pumping process, then the corresponding torus has an odd Z_2 invariant, reflecting the fact that at least one Kramer's pair has "exchanged partners"; the strong topological invariant is finally found as the sum (mod2) of all invariants, whereas the weak indices are given by the Z_2 invariants of tori with the third component being labeled by $n_i = 1$.[6]

$KMgSb_{1-x}Bi_x$ alloys were studied by combining tight-binding parameters obtained via projection onto Wannier functions with the coherent potential approximation (CPA) including self-energy corrections for disorder.[9] Spectral functions shown here have been calculated as $(-1/\pi)\, ImG(\boldsymbol{k};\omega)$, where $G(\boldsymbol{k};\omega) = (\omega - H(\boldsymbol{k}) - \Sigma(\omega) + i\delta)^{-1}$ is the CPA momentum and energy resolved Green's function, and $\Sigma(\omega)$ is the self-energy taking into account all disorder-induced renormalisation effects.

* Electronic address: domenico.disante@spin.cnr.it

[1] G. Kresse and J. Furthmüller, Phys. Rev. B **54**, 11169 (1996).
[2] J. Heyd, G. E. Scuseria, and M. Ernzerhof, J. Chem. Phys. **121**, 1187 (2004).
[3] J. W. Bennett, K. F. Garrity, K. M. Rabe, and D. Vanderbilt, Phys. Rev. Lett. **109**, 167602 (2012).
[4] A. A. Mostofi, J. R. Yates, Y.-S. Lee, I. Souza, D. Vanderbilt, and N. Marzari, Comput. Phys. Commun. **178**, 685 (2008).
[5] J. Henk and W. Schattke, Computer Physics Communications **77**, 69 (1993).
[6] A. A. Soluyanov and D. Vanderbilt, Phys. Rev. B **83**, 235401 (2011).
[7] L. Fu and C. L. Kane, Phys. Rev. B **74**, 195312 (2006).
[8] L. Fu and C. L. Kane, Phys. Rev. B **76**, 045302 (2007).
[9] D. Di Sante, P. Barone, E. Plekhanov, S. Ciuchi, and S. Picozzi, Sci. Rep. **5**, 11285 (2015).

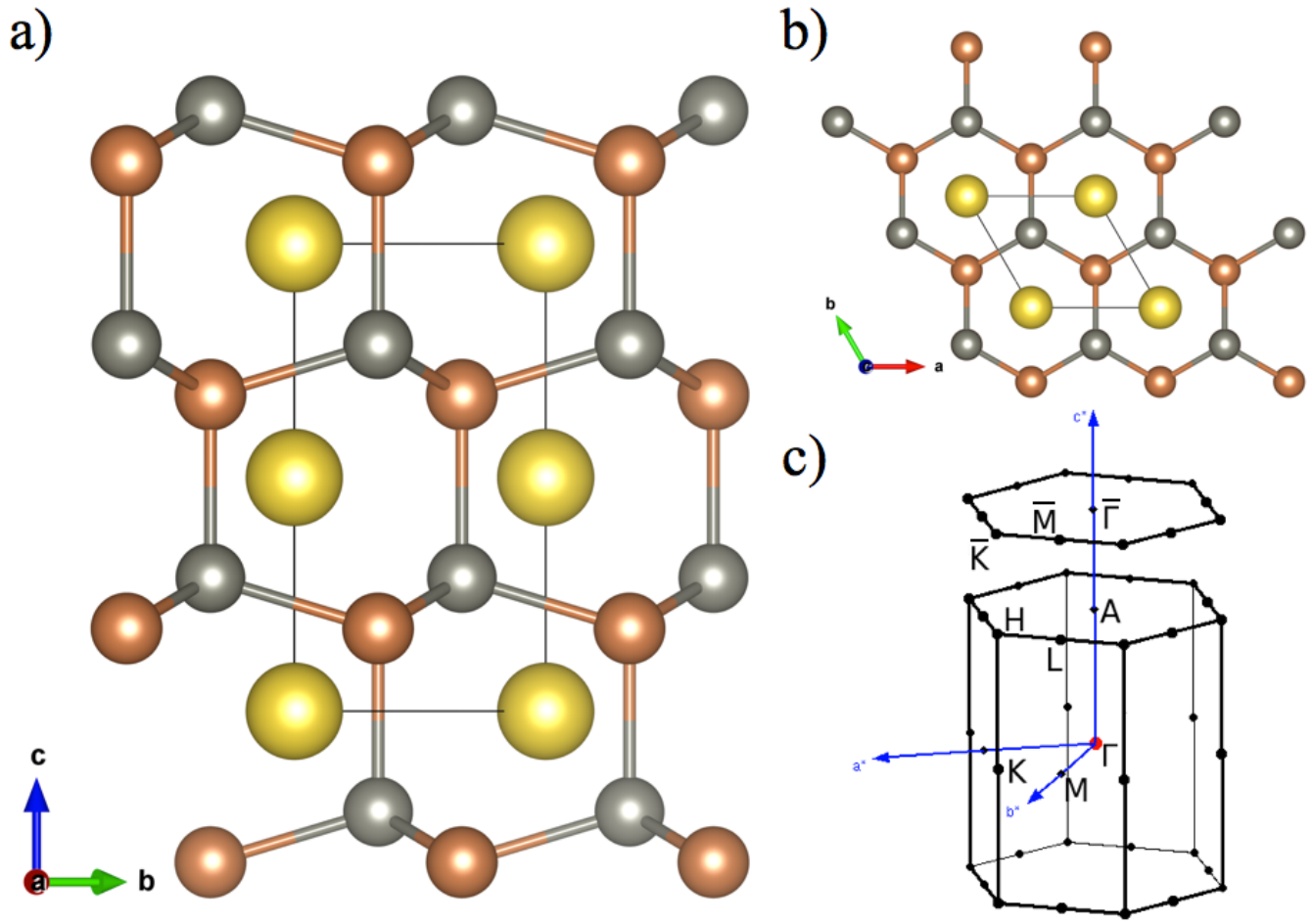

FIG. 1: (Color online) Side view a) and top view b) of LiGaGe-type crystal structures in the low-temperature $P6_3mc$ space group. Yellow, grey and orange balls refer to Li (Na, K), Ga (Zn, Mg) and Ge (Sb, Bi) atoms, respectively. c) Bulk and surface projected Brillouin zone for the structure with the high symmetry points marked.

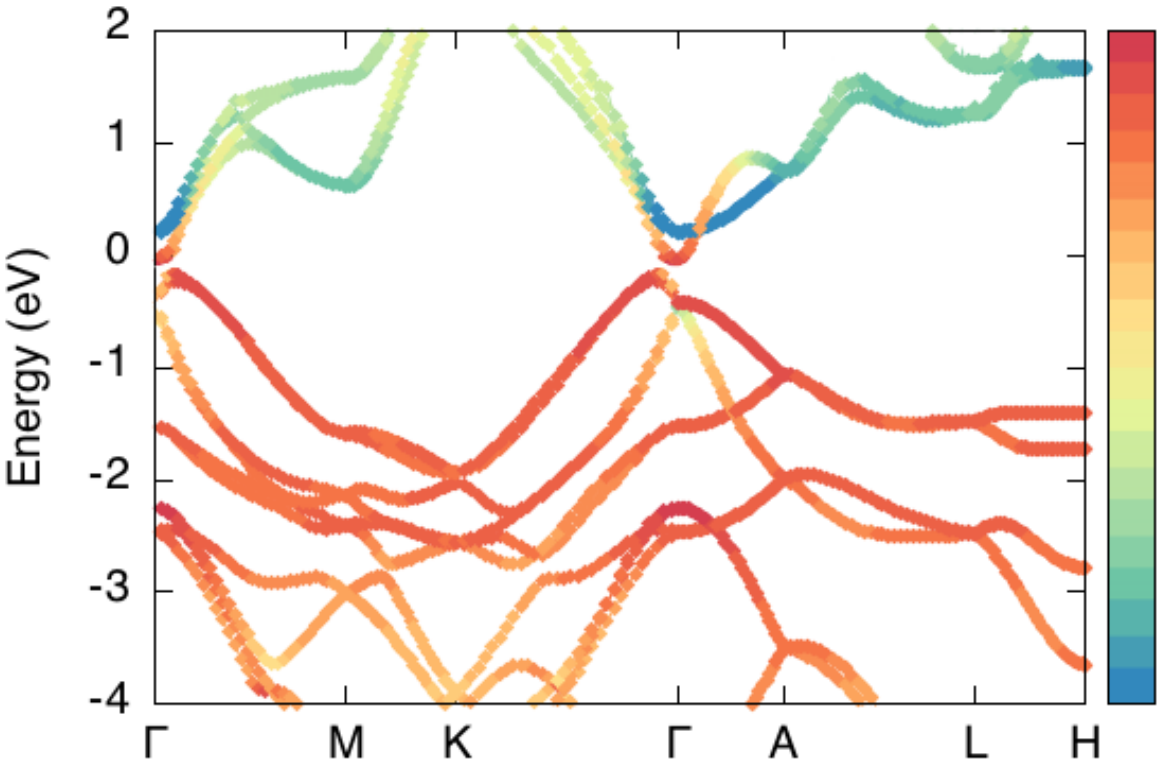

FIG. 2: (Color online) Relativistic bandstructure of KMgBi along the high-symmetry lines of the hexagonal Brillouin zone. Colors highlight the atomic orbital character, from Bi orbitals (red) to an equal mix of Mg and Bi orbitals (blue).

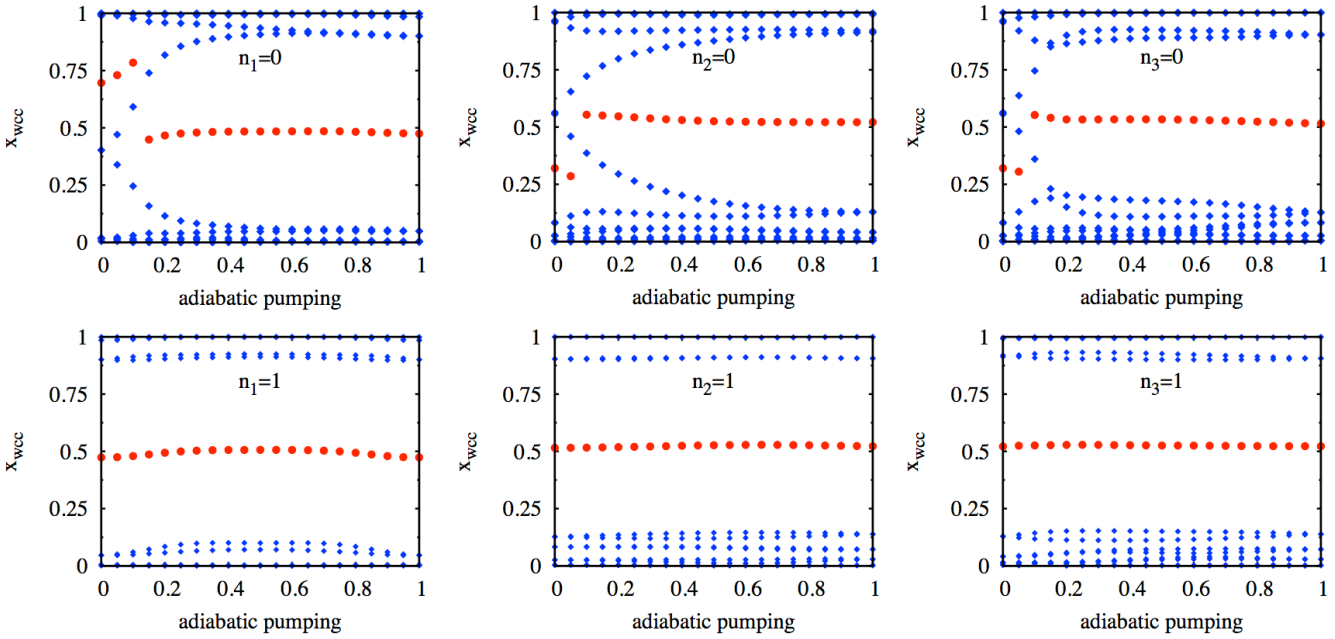

FIG. 3: (Color online) Wannier Charge Centers adiabatic pumping for calculating the topological indexes. KMgBi has a (1;000) index classification, consistently with surface states in Fig. 2c)

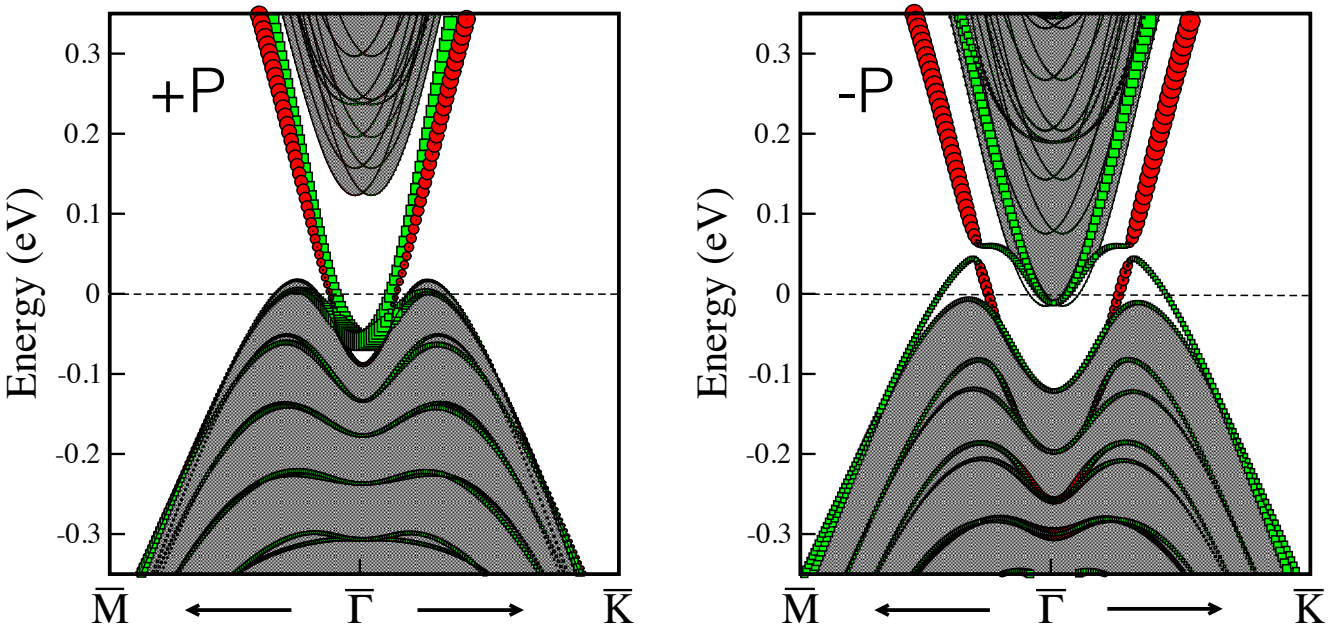

FIG. 4: (Color online) Ab-initio calculations for a 7.6 nm thick slab of KMgBi with opposite directions of the ferroelectric polarization. Within the electrostatic boundary conditions, *i.e* by using a dipole correction that makes vanishing the electric field in the vacuum region, the selfconsistent charge rearrangement due to polar surfaces is fully taken into account. Gray area pictorially highlight the continuum of bulk states, while red and green lines mark contributions from bottom and top terminations of the slab, respectively. The difference in the bulk gap between +P and -P configurations, and in particular the fact that conduction bulk states for -P have been pushed down in energy deforming the Dirac cone from top termination, is a spurious artefact of the used electrostatic boundary conditions (the correct theoretical approach being to impose a vanishing macroscopic electric field $E_{macro} = 0$ in the slab's interior). The strong dependence of the Dirac cones on the polarization direction is clearly visible.

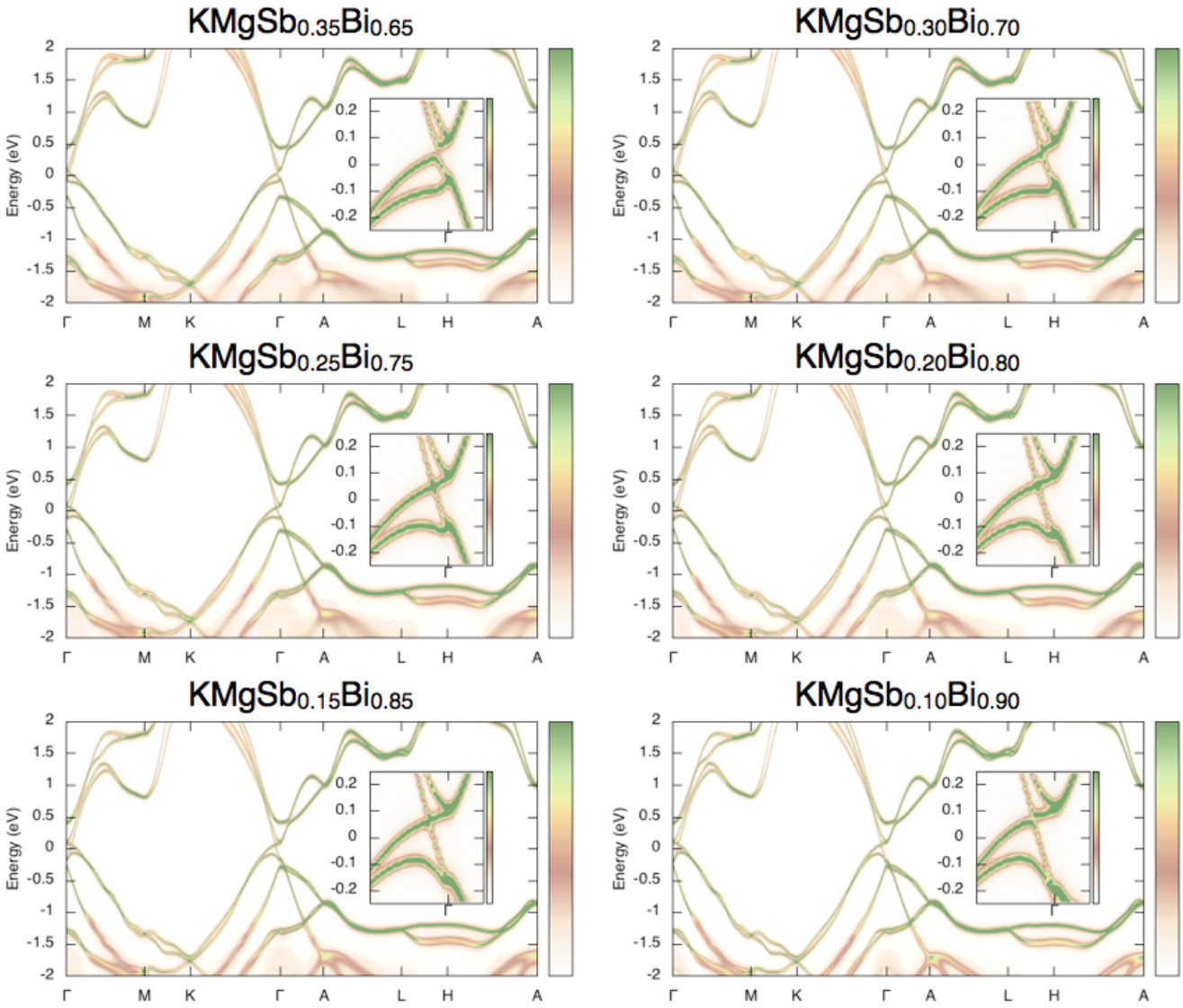

FIG. 5: (Color online) Spectral functions for diluite $KMgSb_{1-x}Bi_x$ alloys at $x = 0.65$, 0.70, 0.75, 0.80, 0.85 and 0.90, respectively. Insets report a zoom around the Fermi level highlighting the Weyl semi-metal phases.